Virtual Synchronous Machine Control for Low-Inertia Power System Considering Energy Storage Limitation

Conference Paper · September 2019

DOI: 10.1109/ECCE.2019.8913169

CITATIONS
10

READS
664

4 authors:

Chu Sun
McGill University
26 PUBLICATIONS **300** CITATIONS
SEE PROFILE

Syed Qaseem Ali
Quanta Technology
41 PUBLICATIONS **529** CITATIONS
SEE PROFILE

Geza Joos
McGill University
417 PUBLICATIONS **16,070** CITATIONS
SEE PROFILE

François Bouffard
McGill University
96 PUBLICATIONS **5,330** CITATIONS
SEE PROFILE

Virtual Synchronous Machine Control for Low-Inertia Power System Considering Energy Storage Limitation

Chu Sun
Department of Electrical and Computer Engineering
McGill University
Montreal, Canada
chu.sun@mail.mcgill.ca

Syed Qaseem Ali
Application eXpertise and Electrical Simulation Division (AXES)
OPAL-RT TECHNOLOGIES Inc.
Montreal, Canada
syed.qaseemali@opal-rt.com

Geza Joos, Francois Bouffard
Department of Electrical and Computer Engineering
McGill University
Montreal, Canada
geza.joos@ mcgill.ca

***Abstract*—The reduced inertia due to integration of power-electronic converters brings about large frequency deviation and rate of change of frequency (ROCOF) in power system which may trigger frequency protection or increase the tears and wears of generators. The existing synthetic inertia and fast frequency response based on renewable energy resource is limited by the unidirectional power reserve, while the emerging virtual synchronous machine (VSM) control is limited by the energy storage needed on DC side. In this paper, an enhanced VSM control is proposed, considering the limitation of energy storage in response speed and energy capacity. The fast -acting energy storage system (FAESS), usually having small energy capacity, is used for emulating inertia and damping. An energy recovery control is proposed so that the energy will be automatically recovered after disturbance, thus reducing the energy capacity needed. The slow-acting energy storage system (SAESS) is controlled like governor control of synchronous machine, which adjusts power based on frequency change, thus taking advantage of its high energy capacity. DC and AC coupling of governor-like control and inertia-damping emulation is proposed, which is unanimous under the scheme of grid-forming and grid-following control. Comprehensive simulation results demonstrated the effectiveness of the proposed control strategy.**

Keywords— Low-inertia power system, frequency control, Inertia-damping emulation, energy recovery control, fast-acting energy storage system, slow-acting energy storage system.

I. INTRODUCTION

The electric power industry is undergoing a revolution towards low-inertia power system with the proliferation of power-electronic integrated DERs, such as wind, photovoltaic (PV) generation and energy storage system (ESS). The reduced inertia will result in high rate of change of frequency (ROCOF) and lower frequency nadir following a contingency event, such as a sudden disconnection of large generation unit or step load change [1]. This also exacerbates frequency fluctuation, thus altering the operational pattern of primary frequency control, leading to more sophisticated regulation efforts and wear-and-tear cost of conventional generation units, for example diesel or hydro generators [2]. The concept of synthetic inertia (SI) is proposed to improve the frequency performance, which can be generally categorized into three types: event-based SI [3], df/dt or frequency deviation based SI [4], or virtual synchronous machine (VSM) [5]. The former two types of SI are majorly based on renewable resource or load which are essentially variable and uncertain, and limited in response speed due to the stability issue due to PLL used in grid-following control [6-8]. In the recent years, there is growing trend of adopting VSM, especially grid-forming VSM which adjusts frequency reference based on local power measurement, to improve frequency regulation [9-10].

The state-of-art review of VSM can be found in [11-12] where different variants of virtual synchronous machine (VSM), like synchronverter, power synchronization converter, robust droop control, etc. are discussed. Though entitled with similar performance as rotational synchronous generator, the energy source on the DC side of VSM to provide frequency response is a main concern. ESS is a promising candidate for VSM application, due to its rechargeable and partially controllable capability [13]. However, there are two intrinsic drawbacks limiting the ESS deployment for conventional VSM.

First, compared with conventional fuel-burnt generator, ESS is limited in power and energy capacity, by which ESS can be generally categorized into two types: short-term and long-term. The state-of-charge (SoC) of battery storage should be maintained with a specific range, for example 20%-90%, to prolong the life cycle and enhance reliability [14]. Second, the performance of SI provided by VSM is subject to the ramping rate or response speed of ESS, by which ESS can be divided into fast-acting ESS (FAESS) and slow-acting ESS (SAESS). Short-term ESS, such as supercapacitor and flywheel, has large power density and can respond very fast, belongs to FAESS, but it usually has small energy density. By contrast, long-term ESS, such as hydrogen storage, electrochemical battery (NaS, Lithium-Ion, PbSO4, etc.) has higher energy density but limited response speed, usually belongs to SAESS [15].

Given the constraints of ESS in energy capacity and response speed, researchers have proposed several improved strategies. In [16], a hybrid energy storage combining battery and supercapacitor is employed to implement VSM where the supercapacitor will tackle the fast-varying power while the battery storage will compensate for the long-term power fluctuation. However, the SoC of super-capacitor is not addressed. The authors of [17] proposed an improved VSM based on type-IV wind turbine generator and short-term ESS whose SoC is managed by additional PI control. However, other types of ESS are not considered in this research. A harmonious integration of FAESS and synchronous generator is introduced in [18] where droop control and SoC feedback (DaSoF) is applied so that ESS can participate in frequency regulation while maintaining SoC around expected value. However, the authors only consider grid following droop control, while most VSM are grid-forming controlled [12].

Considering the research gap of using ESS for frequency support, an enhanced VSM control is proposed with functional roles of both FAESS and SAESS in VSM explored. More specifically, the inertia-damping and governor control of synchronous generator are emulated by FAESS and SAESS respectively, given their difference in response speed and energy capacity. The SoC of FAESS can be secured around specified value with an energy recovery control after inertial response. For generality, both DC-coupled and AC-coupled ESS installation for VSM are also investigated.

II. Power System Studied

The power network studied is shown in Fig. 1, which consists of a synchronous generator (SG), a type-IV wind turbine generator (WTG), active power load and one or multiple energy storage system (ESS). The focus of the research is on active power and frequency control, with reactive power reference for WTG and SG set at zero. The network can correspond to islanded microgrid, small isolated power system or large-area power system. The total inertia of the system is small with high penetration of power-electronic converters, which will be even lower when synchronous generator is unavailable.

III. Proposed Control Strategy

A. Control for DC-Coupled FAESS and SAESS

By carefully comparing the model and control block of synchronous generator with the control philosophy of power converter in AC power system, we find that synchronous generator and its governor is actually a combination of grid forming and grid following control [19]. The inertia and damping part in the synchronous machine control resemble the grid forming control for inverters. When there is a load change, this part will immediately sense the change and adjust frequency. The inertia and damping part are large in power capacity, small in energy capacity, but has fast response. Particularly, the inertia part will not absorb/export power when df/dt is zero and its energy capacity will recover its original value after inertia response. By contrast, the turbine and governor part in the synchronous machine control block are akin to the grid follower control for inverters. This part can act slower but should have larger energy capacity, since the energy of primary (droop) and secondary (integral) control is associated with a longer process.

Based on the above discussion, a VSM control with hybrid ESS is proposed. The FAESS and SAESS are

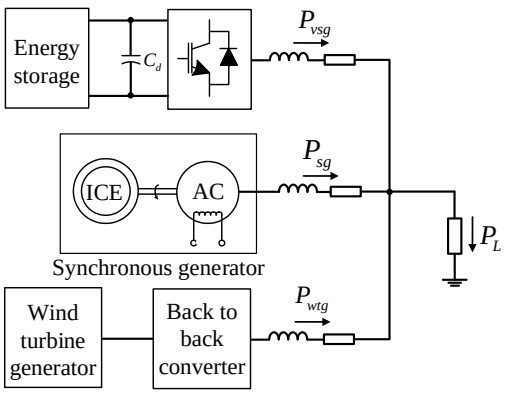

Fig. 1. Configuraiton of the studied power system

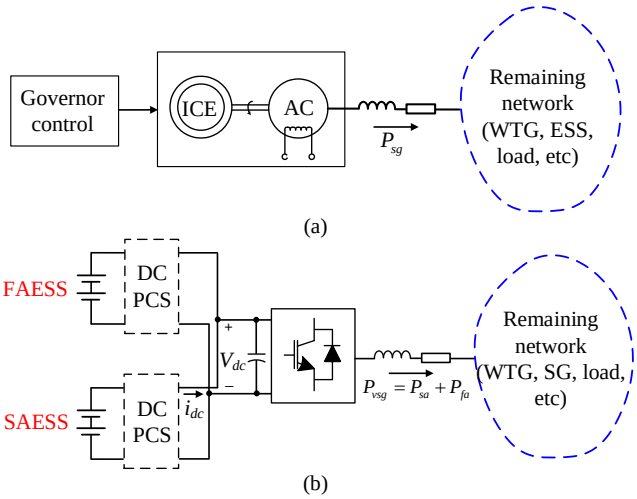

Fig. 2. Diagram of generation units. (a) Synchronous generator with governor control. (b) VSM with DC coupled FAESS and SAESS.

connected in parallel to a common inverter with bidirectional DC power conversion system (PCS). The control strategy of the common inverter will be a combination of both inertia-damping emulation and governor-like control, as with conventional VSM. However, an energy recovery control is also added to the power reference. The energy can be quantified by an SoC-equivalent value of FAESS, such as $CV_{dc}^2/2$ or just DC voltage (V_{dc}) for supercapacitor, $J\omega_r^2/2$ or just rotational speed (ω_r) for flywheel. The typical SoC reference for FAESS will be 0.5.

The DC PCS interfacing FAESS is controlled to maintain constant DC voltage on common DC bus. The DC PCS of SAESS is to follow the power reference from droop and integral control, like the turbine and governor. Therefore, the FAESS will automatically supply the fast-varying components in frequency response, namely the inertia and damping power, while SAESS will track the slow-varying components from the governor control.

B. Control for AC-Coupled FAESS and SAESS

The second type of SG emulation is coupling the inertia and governor parts with two separate inverters. The inverter control for FAESS is to realize inertia-damping performance. An energy recovery control is added to secure the energy of FAESS, by which the average power of FAESS will be zero. The inverter control for SAESS is to realize governor-like control based on droop approach. A secondary integral control using integral block may be also added to recover frequency if the SAESS acts as a slack bus. This inverter will be grid follower, so PLL for grid-synchronization is necessary. After sensing the frequency change, the power reference of SAESS will be adjusted by droop and integral block. The DC PCS interfacing ESS is to maintain the constant DC voltage of inverter, which may be unnecessary for the AC-coupled case.

The AC coupled scheme is more flexible than DC-coupled scheme and conventional synchronous generator. For example, it can be implemented on conventional FACTS devices such as STATCOM or type-IV WTG, with additional FAESS paralleled on the DC bus. Potential participants of VSG may also include electric vehicles (EV), controllable load, HVDC system and wind farms with ESS installed, in certain form of ancillary service.

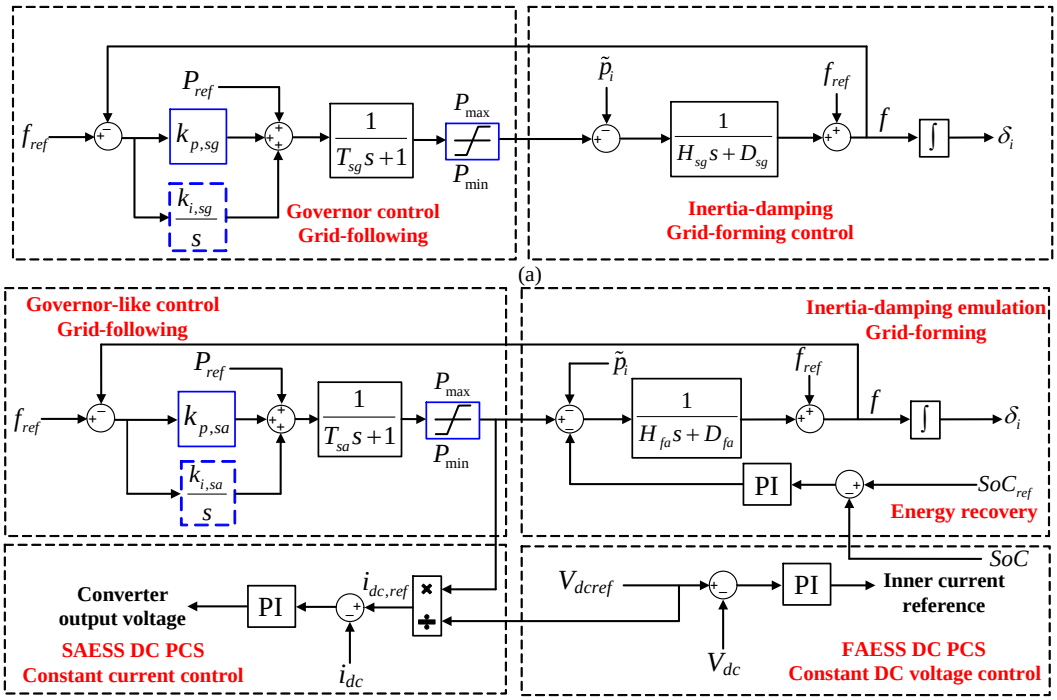

Fig 3. Power and frequency control block (a) Conventional synchronous generator. (b) The DC-coupled hybrid ESS

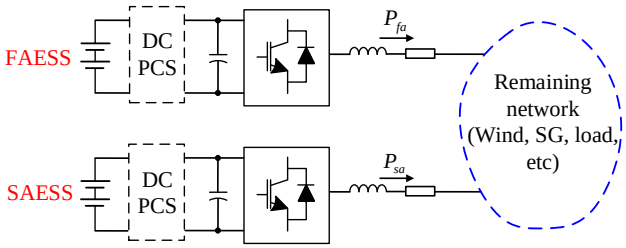

Fig. 4. Diagram of AC-decoupled FAESS and SAESS

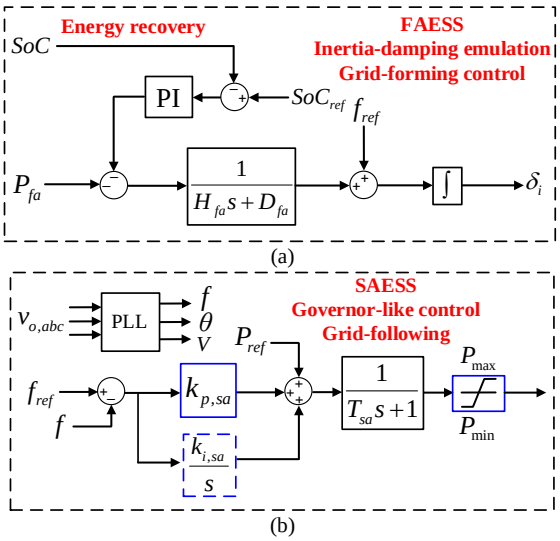

Fig. 5. Control block diagram for AC-coupled FAESS and SAESS. (a) Inertia-damping emulation and energy recovery control of FAESS. (b) Governor-like control of SAESS.

IV. Dynamic Analysis and FAESS Sizing

A. Dynamic Power Sharing between ESS and Generator

Though the control architecture of DC-coupled and AC coupled is different, a uniform approximate analysis is conducted with locational impact of inertia ignored [20]. Given P_{dis} is the total power disturbance from load and renewables, power sharing between FAESS (P_{fa}), SAESS (P_{sa}) and SG (P_{sg}).

$$P_{fa} + P_{sg} + P_{sa} = P_{dis} \tag{1}$$

With governor-like control, the power of SAESS is given by (2), where $k_{p,sa}$ and $k_{i,sa}$ are the parameters of PI controller. The low-pass filters in the conventional governor control loop and locational frequency difference.

$$(k_{p,sa} + \frac{k_{i,sa}}{s})\frac{1}{T_{sa}s+1}(f_{ref} - f) = P_{sa} \tag{2}$$

For the inertia-damping control, the power-frequency relation is given by (3). The power associated with energy recovery control is ignored since it is a slow process.

$$-\frac{1}{H_{fa}s + D_{fa}}(P_{ref,fa} - P_{fa}) = f_{ref} - f \tag{3}$$

For SG, the governor control and inertia-damping effect yields the power-frequency relation as (4) and (5) respectively.

$$-\frac{1}{H_{sg}s + D_{sg}}(P_{ref,sg} - P_{sg}) = f_{ref} - f \tag{4}$$

$$k_{p,sg}\frac{1}{T_{sg}s+1}(f_{ref} - f) = P_{ref,sg} \tag{5}$$

Based on (1)-(5), we obtain the dynamics of system frequency, power of FAESS and SAESS in (6)-(8).

$$f(s) = f_{ref} - \frac{(T_{sg}s+1)(T_{sa}s+1)s}{\left\{\begin{array}{l}((H_{sg}+H_{fa})s + D_{sg} + D_{fa})(T_{sg}s+1)(T_{sa}s+1)s \\ +(k_{p,sa}s + k_{i,sa})(T_{sg}s+1) + k_{p,sg}(T_{sa}s+1)s\end{array}\right\}}P_{dis} \tag{6}$$

$$P_{fa}(s) = (H_{fa}s + D_{fa})(f_{ref} - f(s)) + P_{ref,fa} \tag{7}$$

$$P_{sg}(s) = (k_{p,sg}\frac{1}{T_{sg}s+1} + (H_{sg}s + D_{sg}))(f_{ref} - f(s)) + P_{ref,sg} \tag{8}$$

Therefore, $P_{fa}(s)$ is a high-pass filter (HPF) process while $P_{sa}(s)$ is a low-pass filter (LPF) process. The transient ROCOF and the rate-of-change-of-power (RoCoP) of SAESS can be estimated be (6) and (7). FAESS and SG will share the transient power mismatch in proportion to their inertia values. Therefore, the increased inertia provided by FAESS will reduce both ROCOF and RoCoP, thus relaxing the response speed requirement for SAESS and increasing frequency stability.

$$\frac{dP_{sa}(t)}{dt}\Big|_{t=0} = s^2 P_{sa}(s)\Big|_{s\to\infty} = 0 (T_{sa} \text{ considered})$$
$$\text{or} = \frac{k_{p,sa}}{H_{sg}+H_{sa}} P_{dis} (T_{sa} \text{ ignored}) \quad (9)$$

$$\frac{df}{dt}\Big|_{t\to 0} = s^2 f(s)\Big|_{s\to\infty} = \frac{P_{dis}}{H_{sg}+H_{fa}} \quad (10)$$

$$P_{sg}\Big|_{t\to 0} = sP_{sg}(s)\Big|_{s\to\infty} = \frac{H_{sg}P_{dis}}{H_{sg}+H_{fa}} \quad (11)$$

$$P_{fa}\Big|_{t\to 0} = sP_{fa}(s)\Big|_{s\to\infty} = \frac{H_{fa}P_{dis}}{H_{sg}+H_{fa}} \quad (12)$$

The steady-state power sharing will be $P_{sa}(s\to 0) = P_{dis}$, $P_{af}(s\to 0) = 0, P_{sg}(s\to 0) = 0$. Similarly, we can obtain the power-frequency dynamics when SG is responsible for secondary frequency control while SAESS is employed to emulate droop-based governor control only.

B. Sizing of FAESS

Though larger inertia value is preferred to improve frequency performance, too large inertia will result in slow frequency and energy recovery. Moreover, the synthesized inertia is limited by the energy of FAESS. The energy variation with frequency change can be calculated by (13), where ω_{nom} and $\omega_{\min}$ are the nominal and minimum grid frequency respectively.

$$\Delta E_{\max} = \frac{(J_{fa}\omega_{nom}^2 - J_{fa}\omega_{\min}^2)}{2} \approx J_{fa}\omega_{nom}(\omega_{nom}-\omega_{\min})$$
$$= J_{fa}\omega_{nom}\Delta\omega_{\max} = \frac{J_{fa}\omega_{nom}^2}{2}\frac{\Delta\omega_{\max}}{\omega_{nom}} = H_{fa}S_{nom}\frac{\Delta\omega_{\max}}{\omega_{nom}} \quad (13)$$

The energy variation of prime source is given by

$$\Delta E_{\max} = E_{nom} - E_{\min} = E_{nom}\left(\frac{\Delta E_{\max}}{E_{nom}}\right) \quad (14)$$

Taking supercapacitor as an example of FAESS, the maximum permissible energy released can be calculated by

$$\Delta E_{\max} = \frac{(CV_{dc,nom}^2 - CV_{dc,\min}^2)}{2} \approx CV_{dc,nom}(V_{dc,nom} - V_{dc,min})$$
$$= CV_{dc,nom}\Delta V_{dc,\max} = \frac{CV_{dc,nom}^2}{2}\frac{\Delta V_{dc,\max}}{V_{dc,nom}} \quad (15)$$

Equating (13) with (14) yields the nominal energy E_{nom} required from FAESS to synthesize the given inertia value J as formulated by (16), which implies that E_{nom} equals to the kinetic energy multiplied by the ratio between frequency variation percentage and the energy variation percentage.

$$E_{nom} = H_{fa}S_{nom}\left(\frac{\Delta\omega_{\max}}{\omega_{nom}}\right)/\left(\frac{\Delta E_{\max}}{E_{nom}}\right) \quad (16)$$

Since the energy variation range can be much wider than the frequency variation, for identical inertia value, E_{nom} can be much smaller than the kinetic energy of conventional synchronous generator. This is reasonable considering the decoupling of frequency variation with the primer source energy for inertia emulation. For instance, if the frequency variation is 1% and the energy variation is 10%, the energy required is only 10% relative to conventional kinetic energy.

C. Energy Recovery Loop Design

The simplified SoC control loop is illustrated in Fig. 7 where $G_n(s)$ represents the transfer function from P_{dis} to the power reference of FAESS. To attenuate the effect of SoC control loop on inertia-damping response and frequency regulation, the bandwidth of SoC control loop $G_e(s)$ should be much lower than that of $G_n(s)$. For example, for the control parameters in Table 1, the bandwidth of $G_n(s)$ is 0.325 Hz while the bandwidth of energy control loop $G_e(s)$ is 0.021 Hz, as shown in Fig. 8.

Root locus is used to tune the SoC control parameters. In Fig. 9, the proportional gain ($k_{p,e}$) is kept at 10. With the increasing of integral gain ($k_{i,e}$) from 0.1 to 3, the real part of root is kept constant while the imaginary part increases monotonically. To ensure proper damping, a small integral gain is selected.

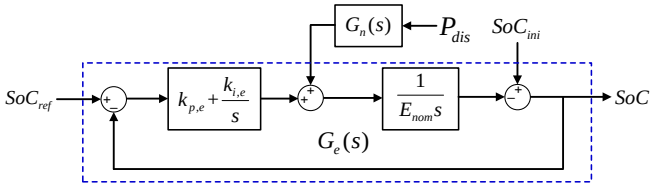

Fig. 6. Simplified diagram of SoC control loop

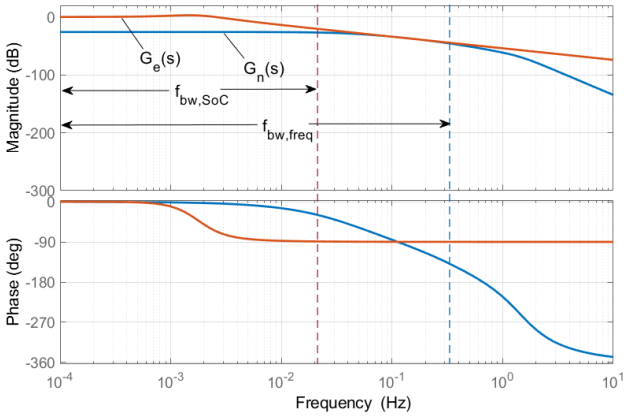

Fig. 7. Simplified diagram of SoC control loop

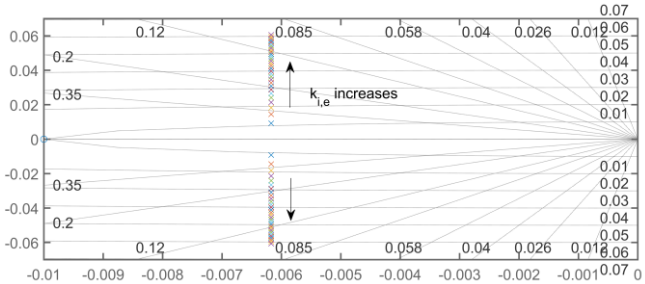

Fig. 8. Root locus of SoC control loop with $k_{i,e}$ varied from 0.01 to 0.3.

V. CASE STUDIES AND RESULTS

The isolated AC system in Fig. 1 is simulated. The parameters are taken from Table 1. Considering the aging process, losses, and duration of energy recovery control, a slightly larger FAESS is adopted, corresponding to the maximum possible H=2700s based on (16) for 1% frequency and 10% SoC variation. WTG adopts MPPT control, and no synthetic inertia and other frequency support from WTG and load are considered.

A. Case 1: DC coupled inertia-damping emulation and governor-like control

The load is increased from 300 kW (0.9375 p.u. with base power S_b at 320 kVA) to 500kW (1.5625 p.u.) at t=15s. In Fig. 9(a), FAESS is unavailable, SAESS adopts frequency PI control, while SG provides small inertia response. The frequency nadir is 58.02 Hz at t=15.32s. The oscillation is also severe due to the interaction between SG and FAESS, with insufficient damping in the system. With FAESS paralleled with SAESS on DC side (P_{ref}=0, H_{fa}=5, D_{fa}=10) but without energy recovery control, frequency nadir is 59.14Hz at t=15.43s, as Fig. 9(b) shows. The oscillation is also signifcantly damped due to the damping term. However, the SoC of FAESS will keep dropping, which is also the case of conventional grid-forming droop controlled inverter or VSM. By contrast, with energy recovery control, SoC of FAESS will return to 0.5 after inertia response, while SAESS will gradually pick up all the power mismatch in steady state, as shown in Fig. 9(c).

Since the inertia and damping of FAESS can be programmed, its effect on dynamic performance can be further investigated. As shown in Fig. 10 (a), with increased inertia (H_{fa}=10s), the frequency nadir rises to 59.27Hz at 15.54s while the ROCOF is drastically decreased. Fig. 10 (b) shows that the oscillation is worsened by smaller damping (D_{fa}=2). Given that conventional synchronous generator has fixed inertia and almost little damping, the control strategy can provide superior control performance. The results for AC-coupled FAESS and SAESS under the same load change

Table 1. Parameters and values of the tested system

Parameters	Values
Base power (S_b)	320 kVA
Power rating of FAESS	320 kVA
Energy capacity of FAESS	24 kWh
SoC$_{ref}$ of FAESS	0.5
Wind speed	10 m/s
Power rating of WTG	250 kVA
Proportional gain of frequency control for SAESS ($k_{p,sa}$)	30
Proportional gain of energy recovery control ($k_{p,e}$)	20
Base frequency (f_{ref})	60 Hz
Power rating of SAESS	320 kVA
Energy capacity of SAESS	360 kWh
Power rating of synchronous generator	320 kVA
Inertia of synchronous generator (H_{sg})	1.2 s
Droop gain of synchronous generator ($k_{p,sg}$)	0.05
Time constant of low-pass filter of governor control (T_{sg})	0.5 s
Integral gain of frequency control for SAESS ($k_{i,sa}$)	20
Integral gain of energy recovery control ($k_{i,e}$)	4

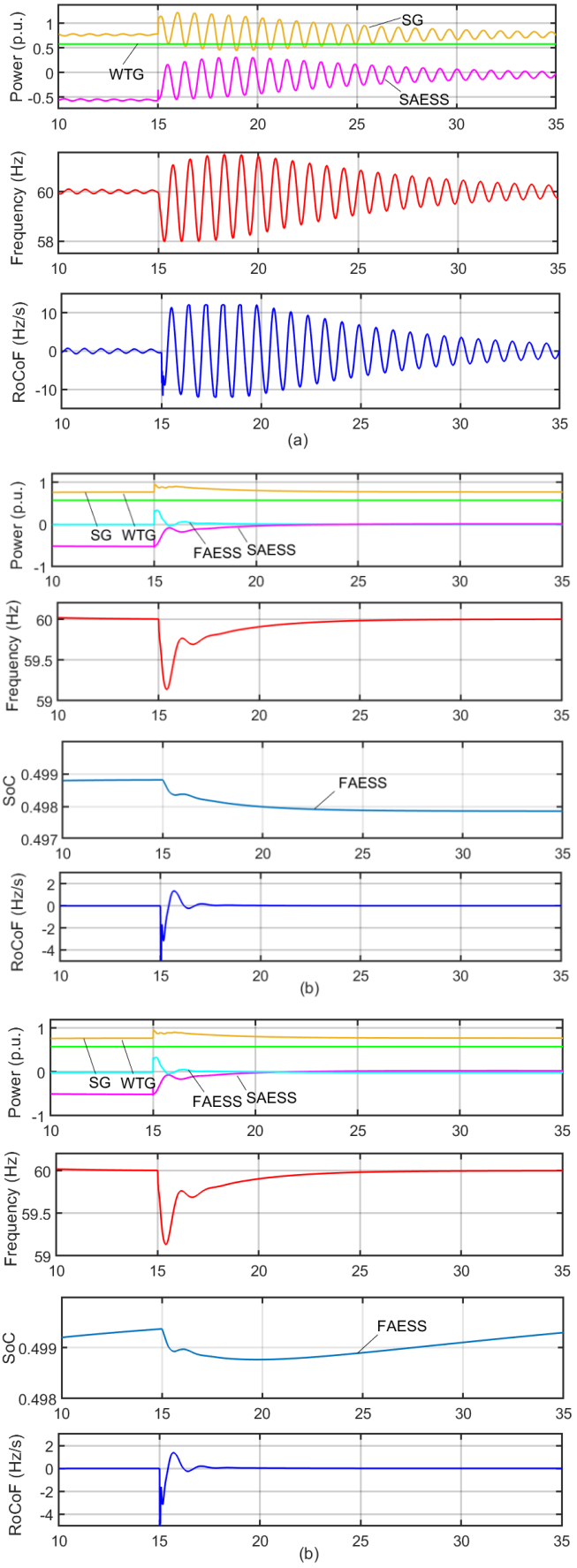

Fig. 9. Results for Case 1. (a) Without FAESS. (b) With FAESS for inertia-damping emulation (H_{fa}=5s, D_{fa}=10) but without energy recovery control. (c) Inertia-damping emulation (H_{fa}=5s, D_{fa}=10) with energy recovery control.

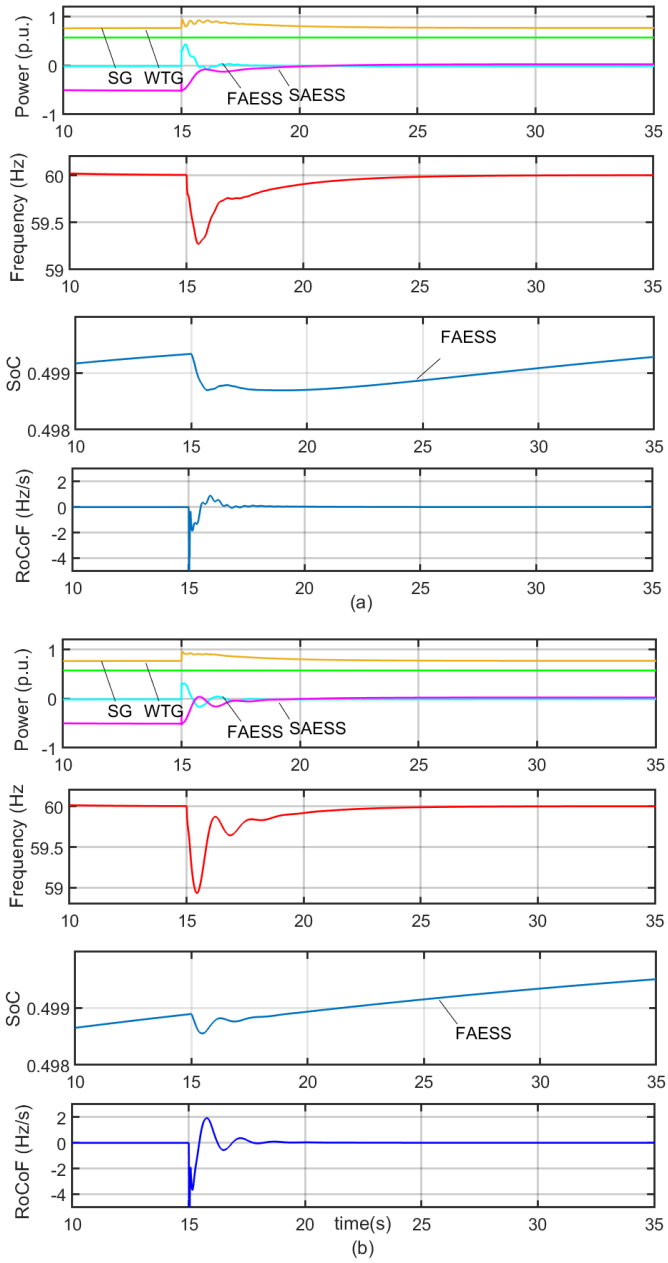

Fig. 10. Results for Case 1 with varied inertia and damping for FAESS (a) Inertia H_{fa}=10s, damping D_{fa}=10. (b) inertia H_{fa}=5s, damping D_{fa}=2.

can be also obtained, which is very close to the results above, thus not given here.

B. Case 2: Diesel generator paralleled with FAESS for inertia-damping emulation

This case study is aimed to test the compatibility of the proposed control strategy with conventional synchronous generator. Frist, a test with only synchronous generator available for frequency control is conducted. PI control is applied to the governor part of diesel generator. For the same load change as Case 1, the frequency nadir is 56.56 Hz at t=15.48s. However, the synchronous generator should respond very fast to maintain power balance, which may be impractical, as Fig. 11(a) shows.

By contrast, when FAESS is available (H_{fa}=5s, D_{fa}=10), the frequency performance becomes much better and SG can respond more slowly in secondary frequency control. Due to energy recovery control, the SoC of FAESS will return to 0.5. As shown in Fig. 11 (b), the power of FAESS gradually decreases to zero and the SoC returns to 0.5. This test shows the compatibility of FAESS control with conventional synchronous generator. Therefore, SAESS used for governor control emulation may be unnecessary if large synchronous generator or other dispatchable resource is available.

C. Case 3: AC coupled scheme for power electronic converter system

Considering a purely power electronic converter system without synchronous generator, the load is increased from 0.9375 p.u. to 1.5625 p.u. at t=15s, as Case 1. Only FAESS in the system can provide inertia response while SAESS will provide primary and secondary frequency control. In Fig. 12(a) where H_{fa}=5, D_{fa}=10 is emulated by FAESS, frequency nadir is 58.88 Hz at t=15.36s, and ROCOF is 6Hz/s. When H_{fa}=10s, D=20 is emulated, frequency nadir increases to 59.29 Hz at t=15.53s, and ROCOF is 3 Hz/s, as shown in Fig. 12(b). The oscillation frequency and the change rate of power of SAESS is also smaller. Therefore, for SAESS with smaller ramping rate limit, the inertia value for FAESS should be

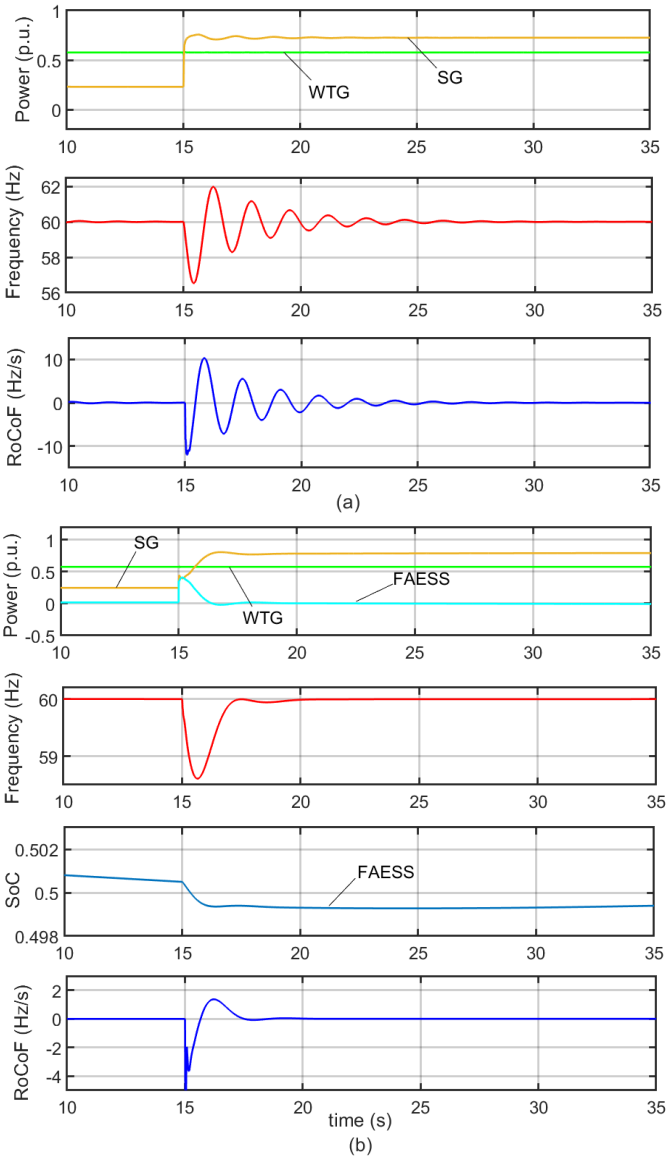

Fig. 11. Results for Case 4. (a) Synchronous generator only. (b) Synchronous generator and FAESS with the proposed inertia-damping emulation (H_{fa}=5s, D_{fa}=10)

larger. With energy recovery control, SoC of FAESS will recover to 0.5, so the SAESS will pick up all the power mismatch in steady state. The results also agree with the theoretical analysis in Section IV.C.

Similarly, in Fig. 12(c), when H_{fa}=5s, D_{fa}=10 are emulated by two FAESS which are the same except small difference in SoC, the frequency nadir and ROCOF are very close to the results in Fig. 12(b). The energy recovery control also effectively makes SoC of the two FAESS recover to 0.5. This implies that with more FAESS installed to emulate the proposed inertia-damping, the equivalent total inertia-damping can be aggregated in the same way as conventional synchronous generators, which shows scalability and flexibility of the AC-coupled scheme of ESS installation.

VI. CONCLUSION

The inertia-damping and governor control of synchronous machine is mapped with grid-forming and grid-following control of power electronic converters in AC power system,

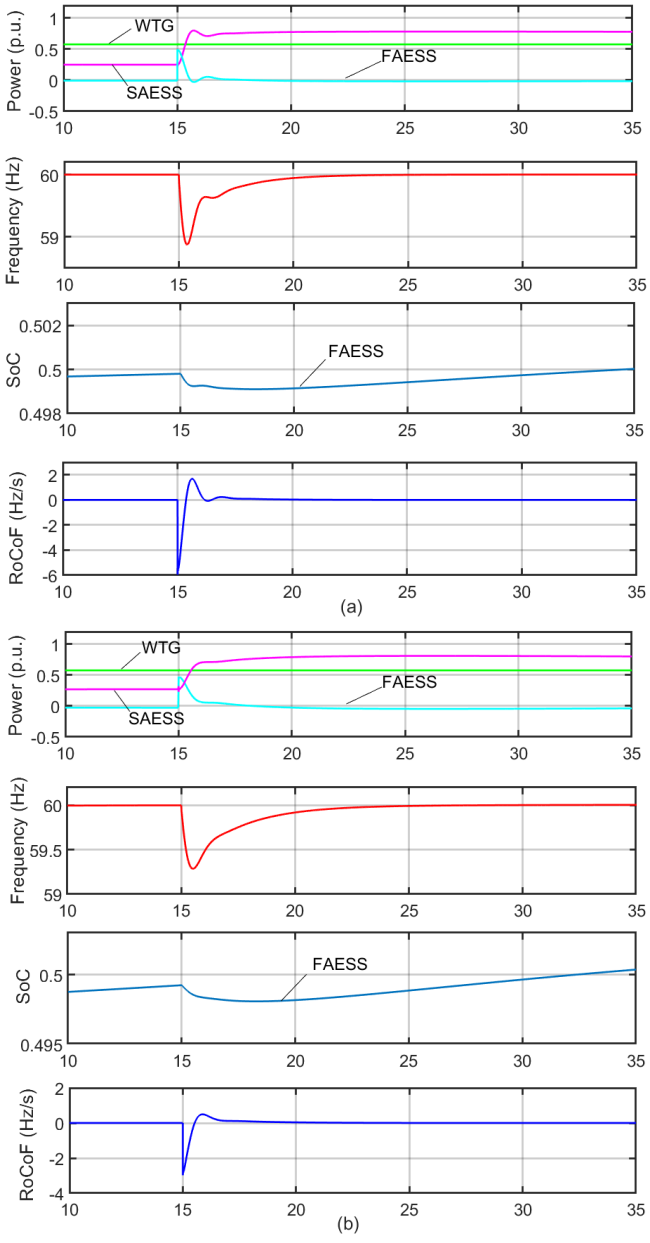

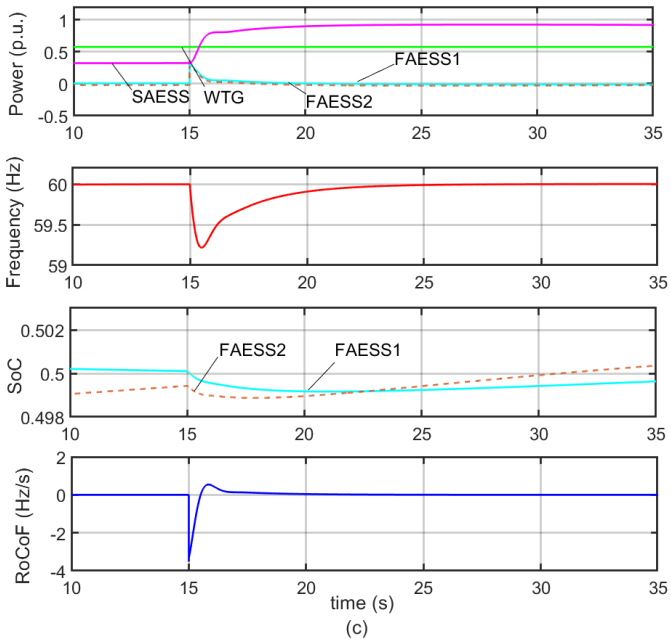

Fig. 12. Power and frequency dynamics in AC coupling case. (a) With one FAESS (H_{fa}=5s and D_{fa}=10) (b) With one FAESS (H_{fa}=10s and D_{fa}=20). (c) With two identical FAESS (H_{fa}=5s and D_{fa}=10).

coupled in the electromechanical process. Therefore, it explains why a single synchronous generator can run autonomously without extra grid former. Based on the analysis, an improved frequency control scheme for inertia-damping emulation and governor-like control is proposed, with the limitation of FAESS and SAESS clarified. The energy recovery control together with inertia emulation applied to FAESS will imitate the real inertia response of synchronous generator. Two types of VSM control implementation are proposed. When DC coupled, the hybrid ESS will have both grid-forming and grid-following function without need of PLL. When AC coupled, the inverter interfaced FAESS can be installed flexibly in the system. With the proposed VSM control, multiple FAESS and SAESS can be placed in different locations of power system, to provide both inertia response and oscillation damping. The control strategy is especially suitable for future power-electronic converter dominated power system featuring low inertia.

REFERENCES

[1] F. M. Uriarte, C. Smith, S. VanBroekhoven and R. E. Hebner, "Microgrid Ramp Rates and the Inertial Stability Margin," in IEEE Transactions on Power Systems, vol. 30, no. 6, pp. 3209-3216, Nov. 2015.

[2] W. Yang, P. Norrlund, L. Saarinen, J. Yang, W. Zeng and U. Lundin, "Wear Reduction for Hydropower Turbines Considering Frequency Quality of Power Systems: A Study on Controller Filters," in IEEE Transactions on Power Systems, vol. 32, no. 2, pp. 1191-1201, March 2017.

[3] S. El Itani, U. D. Annakkage and G. Joos, "Short-term frequency support utilizing inertial response of DFIG wind turbines," 2011 IEEE Power and Energy Society General Meeting, Detroit, MI, USA, 2011, pp. 1-8.

[4] V. Knap, S. K. Chaudhary, D. Stroe, M. Swierczynski, B. Craciun and R. Teodorescu, "Sizing of an Energy Storage System for Grid Inertial Response and Primary Frequency Reserve," in IEEE Transactions on Power Systems, vol. 31, no. 5, pp. 3447-3456, Sept. 2016.

[5] J. Driesen and K. Visscher, "Virtual synchronous generators," 2008 IEEE Power and Energy Society General Meeting - Conversion and Delivery of Electrical Energy in the 21st Century, Pittsburgh, PA, 2008, pp. 1-3.

[6] M. Yu et al., "Instantaneous penetration level limits of non-synchronous devices in the British power system," in IET Renewable Power Generation, vol. 11, no. 8, pp. 1211-1217, 28 6 2017.
[7] D. Duckwitz and B. Fischer, "Modeling and Design of df/dt -Based Inertia Control for Power Converters," in IEEE Journal of Emerging and Selected Topics in Power Electronics, vol. 5, no. 4, pp. 1553-1564, Dec. 2017.
[8] Khan, S.; Bletterie, B.; Anta, A.; Gawlik, W. On Small Signal Frequency Stability under Virtual Inertia and the Role of PLLs. Energies 2018, 11, 2372.
[9] Q. Zhong, "Virtual Synchronous Machines: A unified interface for grid integration," in IEEE Power Electronics Magazine, vol. 3, no. 4, pp. 18-27, Dec. 2016.
[10] Tesla Motors Australia Pty L.td, Market Review-Submission-EPR0053.,2017. [Online] https://www.aemc.gov.au/sites/default/files/content/3e882e74-4416-4c00-9138-81bb5f86f698/MarketReview-Submission-EPR0053-Tesla-Motors-Australia-Pty-Ltd-170420-1.pdf
[11] Tamrakar, U.; Shrestha, D.; Maharjan, M.; Bhattarai, B.; Hansen, T.; Tonkoski, R. Virtual Inertia: Current Trends and Future Directions. Appl. Sci. 2017, 7, 654.
[12] S. D'Arco and J. A. Suul, "Virtual synchronous machines — Classification of implementations and analysis of equivalence to droop controllers for microgrids," 2013 IEEE Grenoble Conference, Grenoble, 2013, pp. 1-7.
[13] I. Serban and C. Marinescu, "Control Strategy of Three-Phase Battery Energy Storage Systems for Frequency Support in Microgrids and with Uninterrupted Supply of Local Loads," in IEEE Transactions on Power Electronics, vol. 29, no. 9, pp. 5010-5020, Sept. 2014.
[14] C. Sun, J. N. Paquin, F. Al. Jajeh, G. Joos and F. Bouffard, "Implementation and CHIL Testing of a Microgrid Control System," *The Tenth Annual IEEE Energy Conversion Congress and Exposition (ECCE 2018)*, Portland, Oregon, 2018.
[15] A. Kusko and J. DeDad, "Short-term, long-term, energy storage methods for standby electric power systems," Fourtieth IAS Annual Meeting. Conference Record of the 2005 Industry Applications Conference, 2005., Kowloon, Hong Kong, 2005, pp. 2672-2678 Vol. 4.
[16] J. Fang, Y. Tang, H. Li and X. Li, "A Battery/Ultracapacitor Hybrid Energy Storage System for Implementing the Power Management of Virtual Synchronous Generators," in IEEE Transactions on Power Electronics, vol. 33, no. 4, pp. 2820-2824, April 2018.
[17] Y. Ma, W. Cao, L. Yang, F. Wang and L. M. Tolbert, "Virtual Synchronous Generator Control of Full Converter Wind Turbines with Short-Term Energy Storage," in IEEE Transactions on Industrial Electronics, vol. 64, no. 11, pp. 8821-8831, Nov. 2017.
[18] J. W. Shim, G. Verbič, N. Zhang and K. Hur, "Harmonious Integration of Faster-Acting Energy Storage Systems into Frequency Control Reserves in Power Grid with High Renewable Generation," in IEEE Transactions on Power Systems, vol. 33, no. 6, pp. 6193-6205, Nov. 2018.
[19] J. Rocabert, A. Luna, F. Blaabjerg and P. Rodríguez, "Control of Power Converters in AC Microgrids," in IEEE Transactions on Power Electronics, vol. 27, no. 11, pp. 4734-4749, Nov. 2012.
[20] T. Xu, W. Jang and T. J. Overbye, "Investigation of inertia's locational impacts on primary frequency response using large-scale synthetic network models," 2017 IEEE Power and Energy Conference at Illinois (PECI), Champaign, IL, 2017, pp. 1-7.